Characterization of the Unbound 2[Fe_4S_4]-Ferredoxin-Like Photosystem I Subunit PsaC from the Cyanobacterium *Synechococcus elongatus*†

Detlef Bentrop,‡ Ivano Bertini,*,‡ Claudio Luchinat,§ Wolfgang Nitschke,|| and Ulrich Mühlenhoff⊥

Department of Chemistry, University of Florence, Via Gino Capponi 7, 50121 Florence, Italy, Department of Soil Sciences and Plant Nutrition, University of Florence, P.le delle Cascine 18, 50144 Florence, Italy, BIP-CNRS, 31, Chemin Joseph Aiguier, 13402 Marseille Cedex 20, France, and Biologisches Institut II, University of Freiburg, Schänzlestrasse 1, 79104 Freiburg, Germany

Received June 11, 1997; Revised Manuscript Received August 7, 1997⊗

ABSTRACT: Recombinant PsaC was reconstituted *in vitro* and investigated by UV/vis, EPR, and ^{1}H NMR spectroscopy. Its UV/vis and EPR spectroscopic properties correspond to those of the wild-type protein. Fast repetition 1D and 2D ^{1}H NMR spectra allowed the sequence-specific assignment of the hyperfine-shifted proton resonances of the cluster-ligating resonances, taking advantage also of chemical shift analogies with other 4 and 8 Fe ferredoxins and a structural model for PsaC. The $C_\alpha-C_\beta-S-Fe$ dihedral angles of the cluster ligands could be estimated from the chemical shifts and relaxation properties of their βCH_2 protons. All NMR-derived structural information on PsaC confirms its similarity to smaller 8Fe ferredoxins serving as electron transfer proteins in solution. Partial reduction of PsaC leads to an intermediate species with strongly exchange broadened ^{1}H NMR resonances. The intermolecular electron exchange rate is estimated to be in the 10^2-10^4 s^{-1} range, the intramolecular electron exchange rate between the two [Fe_4S_4] clusters to be higher than 10^4 s^{-1}. The consequences of these findings for the electron transfer in photosystem I are discussed.

In the photosynthetic electron transport chain of cyanobacteria and higher plants the photosystem I reaction center (PSI hereafter)[1] catalyzes the light-driven electron transfer from cytochrome c_6 or plastocyanin to ferredoxin or flavodoxin [see Golbeck (1994) for a review]. Two structural features are conserved in all type I photosynthetic reaction centers: (i) a membrane-bound homodimeric or pseudo-homodimeric core to which the primary photosynthetic pigment, the intermediate electron-acceptors A_0 and A_1, and the [Fe_4S_4] cluster F_X are bound; (ii) a 2[Fe_4S_4] protein whose iron−sulfur clusters, denominated F_A and F_B, are the terminal electron acceptors of the reaction center.

In PSI, F_A and F_B are harbored by the membrane-associated subunit PsaC. This protein is highly conserved among cyanobacteria, algae, and higher plants and shares similarities with soluble 2[Fe_4S_4] ferredoxins in terms of molecular mass and the presence of two CysXXCysXX-CysXXXCysPro [Fe_4S_4] cluster-binding motives in its primary sequence (Golbeck, 1994). Site-directed mutations of the ligating cysteines of PsaC indicated that cluster F_A corresponds to the C-terminal cluster and F_B to the N-terminal cluster of bacterial 2[Fe_4S_4] ferredoxins (Zhao et al., 1992; Mehari et al., 1995). In all structurally known ferredoxins with two clusters the folding of the polypeptide chain around the [Fe_4S_4] cofactors is very similar (Adman et al., 1976; Stout, 1989; 1993; Duée et al., 1994; Bertini et al., 1995; Moulis et al., 1996). This justifies *a posteriori* the early structural modeling of PsaC based on the X-ray structure of *Peptostreptococcus asaccharolyticus* 2[Fe_4S_4] ferredoxin (Oh-oka et al., 1988a; Dunn & Gray, 1988) despite the low sequence identity between *P.a.* ferredoxin and PsaC (about 19%). Recently, the structure of *P.a.* ferredoxin was modeled into the low-resolution crystal structure of PSI (Krauss et al., 1996).

The three [Fe_4S_4] clusters of PSI (i.e. F_A, F_B, F_X) are clearly visible in the low-resolution crystal structures of PSI from *Synechococcus elongatus* (Krauss et al., 1993, 1996). They form an irregular triangle with one cluster (either F_A or F_B) 15 Å and the other 22 Å apart from cluster F_X and a distance of 12 Å between F_A and F_B within PsaC. The same F_A-F_B separation is observed in dicluster ferredoxins that serve as soluble electron transfer proteins. Due to its low resolution, the X-ray structure of PSI provides no information on which of the two PsaC clusters represents F_A and F_B. On the basis of biochemical evidence obtained by the selective destruction of the terminal clusters, the outermost cluster (22 Å apart from F_X) was tentatively assigned as F_B and a linear flow from F_X via F_A to F_B was proposed (He & Malkin, 1994; Jung et al., 1995). This electron transfer scheme, however, would include a thermodynamic uphill reaction from F_A ($E_m = -520$ mV) to F_B ($E_m = -580$ mV) (Heathcote et al., 1978; Yu et al., 1993), and, in addition, the existence of electron transfer between F_A and F_B has so far not been unambigu-

† Supported by Deutsche Forschungsgemeinschaft (DFG Grant UM 988/2-2 to U.M.), by the European Union, Training and Mobility of Researchers program, with a Large-Scale Facility Grant to I.B. and C.L., and by "Comitato Biotecnologie e Biologia Molecolare" of CNR, Italy.

* To whom correspondence should be addressed. Telephone: +39 55 275 7549. FAX: ++39 55 275 7555. E-mail: bertini@risc1.lrm.fi.cnr.it.

‡ Department of Chemistry, University of Florence.

§ Department of Soil Sciences and Plant Nutrition, University of Florence.

|| BIP−CNRS.

⊥ University of Freiburg.

⊗ Abstract published in *Advance ACS Abstracts,* October 1, 1997.

[1] Abbreviations: PSI, photosystem I; PsaC, subunit VII of photosystem I; 1D, one-dimensional; EPR, electron paramagnetic resonance; *C.p.*, *Clostridium pasteurianum*; *C.au.*, *Clostridium acidi-urici*, *P.a.*, *Peptostreptococcus asaccharolyticus* (formerly *Peptococcus aerogenes*).

S0006-2960(97)01405-0 CCC: $14.00

ously demonstrated. Detailed kinetic analyses of the electron transfer reactions around the iron−sulfur clusters at room temperature have so far been precluded by the fact that these centers cannot be unambiguously distinguished by standard spectroscopic techniques [see Brettel (1997) for a review]. Recent photoelectric measurements on oriented PSI particles, however, which were interpreted as to include linear electron transfer reactions from F_X via F_B to F_A, point toward the existence of linear forward electron flow between the three iron−sulfur clusters of PSI (Sigfriedsson et al., 1995; Leibl et al., 1995).

Over the last years, NMR spectroscopy has become a powerful tool for the investigation of iron−sulfur electron transfer proteins. The information that can be obtained ranges from the identification of the positions of the Fe^{2+} and Fe^{3+} ions in $[Fe_4S_4]^{3+}$ clusters to solution structure determination (Banci et al., 1993; Bertini & Luchinat, 1996a,b; Babini et al., 1996; Bertini et al., 1996). In the case of dicluster ferredoxins, additional information on the intra- and intermolecular electron transfer in the one-electron reduced form can be obtained from exchange spectroscopy (EXSY) on partially reduced samples, as demonstrated for *C. pasteurianum* 2[Fe_4S_4] ferredoxin (Bertini et al., 1990, 1992). For the same protein, early ^{13}C NMR measurements permitted to calculate the difference of the redox potential of the two clusters (Packer et al., 1975).

The present study of reconstituted, unbound PsaC from PSI aims at the spectroscopic characterization of this important subunit of PSI in order to obtain structural information and to gain a better understanding of the two clusters F_A and F_B with respect to their function for the electron transfer from F_X to the soluble acceptor protein ferredoxin or flavodoxin.

MATERIALS AND METHODS

Expression of the PsaC Apoprotein

The genomic Sau3AI fragment from *S. elongatus* carrying the psaC gene (EMBL accession No. X63767) was modified by polymerase chain reaction using a modifying primer (TTACTCCATGGCTCACACTG) and the T7-primer to create an *Nco*I restriction site at the start codon. The fragment was inserted into the *Nco*I and *Bam*HI restriction sites of the *Escherichia coli* expression vector pET15b (Studier et al., 1990). The correctness of the construct was verified by DNA sequencing. PsaC was expressed in *E. coli* strain BL21(DE3) growing in media M9ZB supplemented with 50 μM $FeCl_3$ as described previously (Studier et al., 1990). Cells were harvested by centrifugation 5 h after induction with 1 mM isopropyl β-D-thiogalactoside, washed in TS buffer (50 mM Tris, 100 mM NaCl, 2 mM EDTA, pH 8.0), resuspended in TS buffer, and broken by two cycles in a french pressure cell at 700 bar. The brown inclusion bodies were collected by centrifugation and separated from the bulk membranes by repetitive centrifugation through a 10% sucrose cushion in TS buffer at 1500*g* for 10 min. The inclusion bodies were solubilized for 1 h at room temperature in 50 mM Tris (pH 8.0) containing 6.8 M urea and 1% mercaptoethanol as described, and insoluble material was subsequently removed by centrifugation (Li et al., 1991). PsaC apoprotein was purified by FPLC gel filtration chromatography on a 1.6 × 70 cm Sephadex G-100 column in TS buffer containing 6.8 M urea and 0.1% mercaptoethanol at room temperature and concentrated by ultrafiltration on a YM3 membrane (Amicon). At this step a pure apoprotein was obtained as judged by SDS−polyacrylamide gel electrophoresis. Approximately 20 mg of purified apoprotein was routinely obtained from 1 L of culture.

Reconstitution and Purification of PsaC

All subsequent steps were performed under anaerobic conditions in a glove box containing an oxygen-free methane/hydrogen atmosphere. PsaC apoprotein was made anaerobic by storage in an oxygen-free atmosphere for at least 12 h and the iron−sulfur centers were subsequently reconstituted essentially as described previously (Mehari et al., 1991): the denatured protein was diluted to a final concentration of about 10 μg/mL in oxygen-free 50 mM Tris (pH 8.3) and 1% mercaptoethanol. Subsequently, $FeCl_3$ was added to a final concentration of 0.3 mM followed by addition of Na_2S to a final concentration of 0.3 mM. The reconstitution mixture was allowed to incubate anaerobically in darkness for at least 16 h.

For purification of the holoprotein, the reconstitution mixture was applied to a 25 mL Q-Sepharose ion-exchange column equilibrated with buffer A (25 mM sodium phosphate, pH 8.0, 0.1% mercaptoethanol) under anaerobic conditions. The column was washed with buffer A containing 0, 100, and 175 mM NaCl, and PsaC was subsequently eluted by a step of 250 mM NaCl in buffer A. The brown-yellow protein solution was excessively concentrated by ultrafiltration under nitrogen to concentrations of 1−2 mM, shock-frozen, and stored in liquid nitrogen until further use. Solvent exchange to D_2O, as desirable for NMR spectroscopy, was performed by repetitive dilution of the concentrated sample with deuterated buffer A containing 250 mM NaCl followed by ultrafiltration. To estimate the protein concentration, an extinction coefficient of $E_{400} = 6000\ M^{-1}\ cm^{-1}$ was used (Armengaud et al., 1995) for the reconstituted PsaC and $E_{275} = 9500\ M^{-1}\ cm^{-1}$ was employed for the holoprotein. The latter coefficient was calculated from the amino acid sequence (Mühlenhoff et al., 1993).

EPR Spectroscopy

EPR spectra were recorded on a Bruker ESP300E X-band spectrometer fitted with an Oxford Instruments liquid helium cryostat and temperature control system.

NMR Spectroscopy

Several samples of reconstituted PsaC were used for the NMR experiments with protein concentrations ranging from 1 to 1.5 mM. The protein was dissolved in buffer A containing 250 mM NaCl in 99.9% D_2O (pH uncorrected for the deuterium isotope effect). One sample was in the same buffer in 90% H_2O/10% D_2O. All sample handling was done anaerobically under an argon atmosphere. Reduction of PsaC was accomplished by addition of aliquots of freshly prepared 25 or 50 mM sodium dithionite in degassed 0.2 M sodium phosphate (pH 8) or by addition of a small amount of solid sodium borohydride to the protein solution. Benzyl viologen was also dissolved in 0.2 M sodium phosphate (pH 8) prior to addition to the NMR tube. If necessary, a 1 M potassium phosphate buffer (pH 10.5) was used to adjust the pH of the sample solution.

All ^{1}H NMR spectra were recorded on Bruker spectrometers working at a proton resonance frequency of either 500 or 600 MHz (DRX 500 or AMX 600). 1D spectra were generally acquired with a superWEFT pulse sequence (Inubushi & Becker, 1983). 1D NOE difference spectra were obtained upon selective irradiation of hyperfine shifted, fast relaxing signals of oxidized PsaC according to previously described acquisition schemes (Johnson et al., 1983; Banci et al., 1989) in D_2O solution using irradiation times of 95 ms and a repetition rate of 5.4 s^{-1} over a spectral window of 32 ppm. Non-selective T_1 relaxation times were derived from an exponential three-parameter fit of the data obtained in a series of inversion recovery experiments (Vold et al., 1968) with delays from 0.25 to 150 ms. Two fast repetition WEFT-NOESY (Chen et al., 1994) spectra for the detection of dipolar connectivities of the hyperfine shifted signals were recorded at 300 K over a spectral window of 34 ppm with the following parameters: (i) 10 ms mixing time, 4K data points in *F*2, repetition rate 2.4 s^{-1}, 256 increments in *F*1, 512 transients per increment; (ii) 5 ms mixing time, 2K data points in *F*2, repetition rate 5.4 s^{-1}, 256 increments in *F*1, 1K transients per increment. The data matrices of these 2D spectra were processed to a final size of 1K × 1K data points using shifted squared sine window functions prior to Fourier transformation.

To facilitate the assignment of the observed NOEs between the hyperfine shifted signals and resonances in the diamagnetic shift range, several standard ^{1}H 2D NMR spectra were recorded over a spectral window of 12.7 ppm at 300 K in D_2O solution [DQF-COSY (Rance et al., 1983), CLEAN-TOCSY (Griesinger et al., 1988) with 30 and 80 ms spin-lock mixing time, and a 30 ms NOESY (Wider et al., 1984), each with 4K data points in *F*2 and 512 increments in *F*1]. They were processed to a final size of 2K × 1K data points. Phase sensitivity was achieved for all 2D spectra by application of the TPPI scheme (Marion & Wüthrich, 1983). All NMR spectra were calibrated assuming a chemical shift of 4.79 ppm for the residual water signal at 300 K with respect to DSS and processed with the standard Bruker software.

Structural Model of PsaC

A structural model of PsaC was built on the basis of the high-resolution X-ray structure of the 2[Fe_4S_4] ferredoxin from *Clostridium acidi-urici* (Duée et al., 1994) (PDB entry 1FDN). Appropriate mutations, an insertion of 8 amino acids between Gly 26 and Asp 27 of *C.au.* ferredoxin, and a short N-terminal as well as a long C-terminal extension were introduced by means of the program SYBYL (Tripos Assoc.). The resulting structure was energy minimized *in vacuo* using the AMBER4.0 (Pearlman et al., 1991) program package. During the energy minimization the positions of the cluster ligating cysteines and of the two iron−sulfur clusters were kept fixed. The minimized structural model was used as input for the program PROCHECK (Laskowski et al., 1993). It was found to exhibit satisfying Ramachandran plot statistics and side chain geometries.

RESULTS

Characterization of the Recombinant PsaC Holoprotein

The UV/vis spectrum of purified reconstituted PsaC shows a broad maximum at 390 nm and a broad shoulder at 320 nm (Figure 1A) similar to those of typical 2[Fe_4S_4] ferredoxins (Armengaud et al., 1995). The spectral ratio A_{390}/A_{280} is 0.65, a value similar to PsaC purified from spinach thylakoids (Oh-oka et al., 1988a). Upon reduction with sodium dithionite at pH 8.0, the absorption in the entire visible region is decreased and the broad spectrum typical of fully reduced ferredoxins is observed (not shown). This effect is reversed in contact with air. The EPR spectrum of the recombinant protein in the fully reduced state is shown in Figure 1B. Very similar EPR spectra, although with drastically reduced intensity, were obtained from the PsaC inclusion bodies, indicating that they contain insoluble PsaC with partially assembled iron−sulfur clusters (not shown). The spectrum in Figure 1B closely resembles those reported previously for PsaC purified from spinach PSI (Oh-oka et al., 1988b; Mehari et al., 1991). Cluster reconstitution experiments performed on the isolated spinach PsaC resulted in significant line broadening and hence less well-resolved

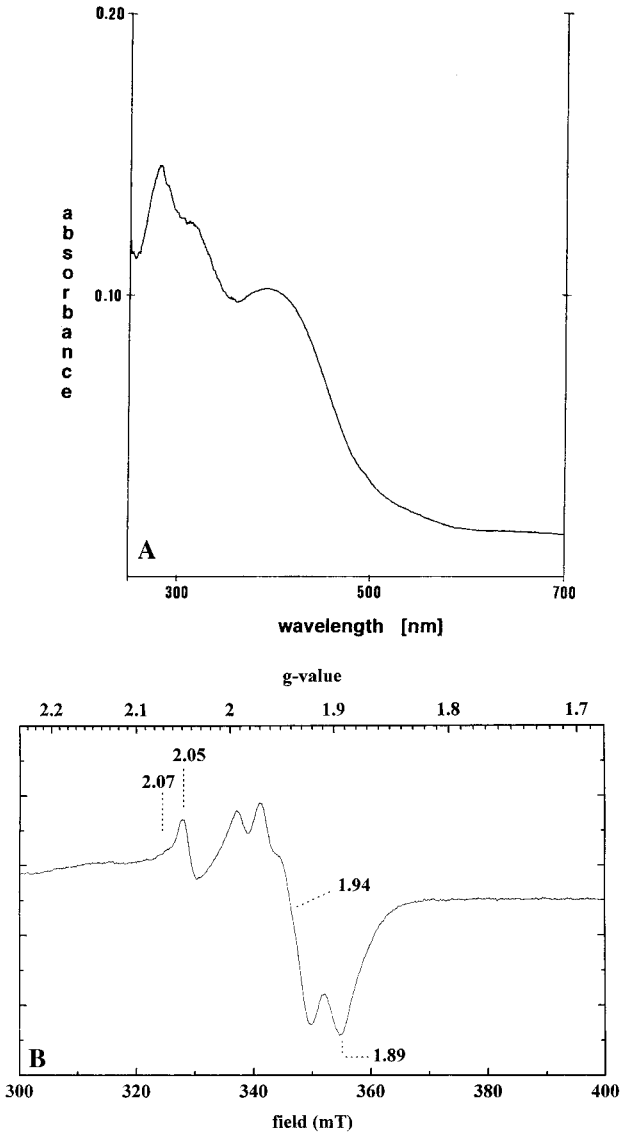

FIGURE 1: UV/Vis (panel A) and EPR spectrum (panel B) of reconstituted recombinant PsaC from *S. elongatus*. The UV/vis spectrum was recorded in the oxidized state, and the EPR spectrum was recorded in the fully reduced state. Complete reduction of PsaC was achieved by adding 5 mM sodium dithionite at pH 10.0. Instrument settings for the EPR experiment: temperature, 15 K; microwave power, 6.7 mW; microwave frequency, 9.42 GHz; modulation amplitude, 1 mT.

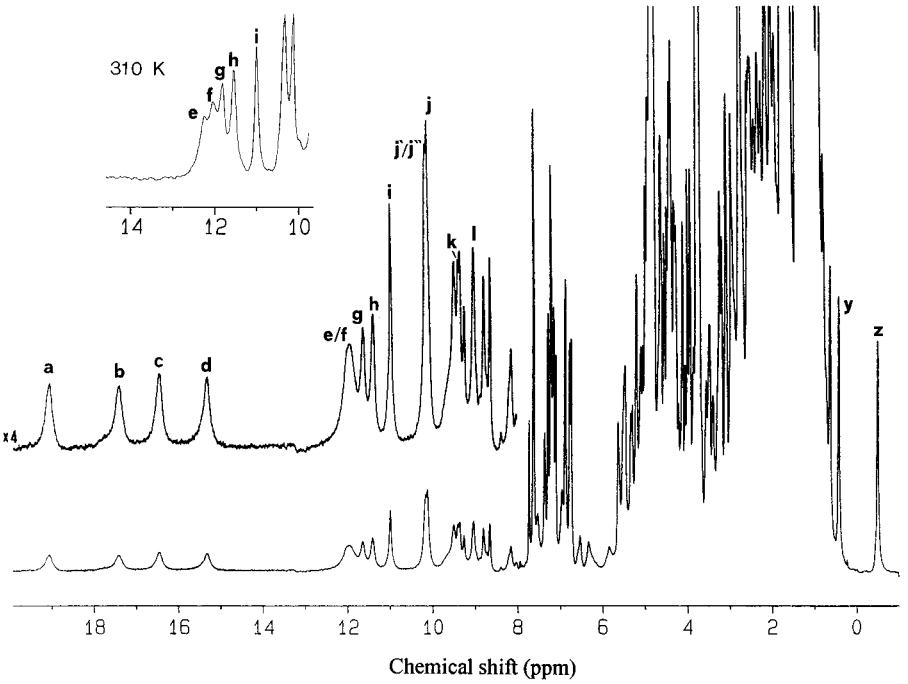

FIGURE 2: 600 MHz 1D ^{1}H NMR spectrum of oxidized PsaC from *S. elongatus* [recorded at 298 K in 25 mM sodium phosphate (pH 8.0), 250 mM NaCl, 0.1% mercaptoethanol in 99.9% D_2O] shows a set of downfield-shifted resonances that are typical for 8Fe ferredoxins. The small inset shows the partial resolution of signals **e** and **f** at 310 K.

EPR spectral features (Mehari et al., 1991). This line broadening was interpreted as being due to an increased conformational heterogeneity. The similarity of the spectrum in Figure 1B to those reported for the isolated protein from spinach and to those obtained on PsaC inclusion bodies shows that cluster reconstitution into recombinant PsaC does not induce increased heterogeneity as compared to the unpurified, unreconstituted protein.

The long-term stability of the holoprotein was investigated by comparison of the UV/vis spectra of the protein after storage under different conditions. For determination of pH effects, samples were stored anaerobically in 100 mM buffer containing 250 mM NaCl and 0.1% mercaptoethanol. The protein was found to be very sensitive to low pH: samples stored at room temperature in darkness at pH 5.0, 6.0, and 6.5 deteriorated completely within 12 h. At pH 7.0 and 7.5, 85% of the absorbance maximum at 390 nm remained after 4 days. For pH values above 7.5, more than 90% of the absorption maximum was still present after 2 weeks independent of the nature of the buffer. The presence of mercaptoethanol was also found to be beneficial to the protein stability. In its absence A_{390} declined to 85% after 3 days. Similar values were obtained in the presence of 1.7 mM ascorbic acid. NaCl was found to be essential for the stability as PsaC deteriorated rapidly upon dialysis against NaCl-free buffer while samples were found to be stable in the presence of 100−400 mM NaCl. The protein is oxygen-sensitive: a completely anaerobic sample starts to decompose in contact with air after 3−4 h.

^{1}H NMR Spectroscopy on Oxidized PsaC

The 298 K ^{1}H NMR spectrum of oxidized PsaC in D_2O solution (uncorrected pH = 8) displays eight signals in the 11−20 ppm region (Figure 2; labeled **a**−**h**). They can be readily attributed to βCH_2 protons of its eight cysteinyl cluster ligands due to the hyperfine contribution to their chemical shifts and relaxation properties [T_1 values in the 5−10 ms range (Table 1)], due to the strong temperature dependence of their chemical shifts (uniformly of the anti-Curie type as expected for oxidized [Fe_4S_4] proteins; see Supporting Information) and due to the fact that they are not solvent exchangeable. In the high-field region, the PsaC

Table 1: Assignment and Properties of the Hyperfine Shifted Resonances of Oxidized PsaC

cysteine[a]	signal[b]	δ[c] (ppm)	T_1 (ms)	assignment		cluster[d]
Cys A (Cys II)	**a**	19.1	8.3	Hβ_2	Cys 50	F_A
	l	9.04	13.6	Hβ_1		
	i	10.98	26.6	Hα		
Cys B (Cys II)	**b**	17.4	6.3	Hβ_2	Cys 13	F_B
	k	9.49	10.8	Hβ_1		
	j	10.10	21[e]	Hα		
Cys C (Cys III)	**c**	16.5	7.6	Hβ_1	Cys 53	F_A
		5.5	nd[f]	Hβ_2		
		6.95	nd[f]	Hα		
Cys D (Cys III)	**d**	15.4	7.2	Hβ_1	Cys 16	F_B
		6.3	nd[f]	Hβ_2		
		7.52	nd[f]	Hα		
Cys E (Cys I)	**e**	12.0	5.2[g]	Hβ_1	Cys 47	F_A
	j′	10.17	8.5[e,g]	Hβ_2		
Cys F (Cys I)	**f**	12.0	5.2[g]	Hβ_1	Cys 10	F_B
	j″	10.17	8.5[e,g]	Hβ_2		
Cys G (Cys IV)	**g**	11.7	8.3	Hβ_2	Cys 57[h]	F_B[h]
		9.65	nd[f]	Hβ_1		
Cys H Cys (IV)	**h**	11.4	10.3	Hβ_2	Cys 20[h]	F_A[h]
		8.8	5[e]	Hβ_1		

[a] The classification with roman numerals refers to the position of the cysteine residue in the common cluster binding sequence motif ···C(I)xxC(II)xxC(III)···C(IV)P···. [b] The letter code is the same as for Figure 2. [c] Chemical shifts are given at 300 K. [d] Cluster F_A of photosystem I is the C-terminal cluster of PsaC and cluster F_B is the N-terminal one. [e] Value was estimated from the null point in inversion recovery experiments. [f] nd, not determined. [g] Apparent T_1 relaxation time of overlaid signals. [h] Assignment is tentative.

spectrum exhibits two well-resolved resonances (**y**, **z**), each with three-proton intensity strongly indicative of methyl groups.

Connectivities between the βCH_2 protons and partially also with the Hα protons of the cluster-ligating cysteines were identified in 1D NOE difference experiments on the hyperfine shifted resonances (see Supporting Information) and fast repetition NOESY spectra with short mixing time (≤10 ms) (data not shown). Signal **a** shows dipolar connectivities with signals **i** (10.98 ppm) and **l** (9.04 ppm) as well as a weak NOE with a resonance at 1.20 ppm. The assignment of **l** as geminal and of **i** as vicinal partner of **a** is based on the relative intensities of the 1D NOEs and the longer T_1 relaxation time of **i**, indicative of a Hα (Table 1). Irradiation of **i** yields only a NOE to signal **l**. Resonance **b** correlates in a dipolar fashion to resonance **j** (10.10 ppm), **k** (9.49 ppm), and weakly to a signal at 1.23 ppm. Following the same arguments as above, **k** is assigned to the geminal and **j**, with the longer T_1 and the weaker NOE, to the vicinal partner of **b**. It should be noted that both of the cysteines represented by **a** and **b**, respectively, are characterized by a Hα proton with a chemical shift downfield of the second Hβ proton and a considerably longer relaxation time than the βCH_2 protons. Such a pattern is generally observed for cysteine ligands II and III in oxidized [Fe_4S_4] ferredoxins (Donaire et al., 1994) since they have the Hα pointing away from the cluster as known from X-ray crystallography (Adman et al., 1976; Stout, 1989; Duée et al., 1994; Moulis et al., 1996; Fukuyama et al., 1988; Kissinger et al., 1991; Sery et al., 1994; Macedo-Ribeiro et al., 1996) and solution structure determination (Bertini et al., 1995).

Irradiation of signal **c** yields a weak NOE to **d** clearly identifying these two signals as belonging to the two Cys III cluster ligands. The available structural data on dicluster ferredoxins suggest that only these cysteines are close enough in space to allow for a NOE between a Hβ of Cys III of cluster I and a Hβ of Cys III of cluster II (Adman et al., 1973, 1976; Stout, 1989; Duée et al., 1994). This feature of 7Fe and 8Fe ferredoxins reflects their highly conserved internal pseudo 2-fold symmetry which is also known to be maintained in PsaC from the low-resolution X-ray diffraction data on PSI (Krauss et al., 1996). The further dipolar connectivities of **c** [NOEs with resonances at 6.95, 5.5 (broad), 1.33, 1.11, and 0.73 ppm] are consistent with its assignment to one βCH_2 proton of a cysteine III ligand. Its geminal partner can be assigned to the resonance at 5.5 ppm and the corresponding Hα to 6.95 ppm due to chemical shift analogy with *Clostridium pasteurianum* type 8Fe ferredoxins (Bertini et al., 1994) and the above mentioned general property of the chemical shift ratios in oxidized 4Fe and 8Fe ferredoxins (i.e. moderately relaxed Hα of cysteines II and III downfield of the second Hβ). The 1D NOE difference spectrum of signal **d** is similar to that of **c**. It exhibits resonances at 7.52 ppm (assigned to the vicinal partner of **d**), 6.95 ppm (the Hα of Cys C), and 6.3 ppm (broad, assigned to the second Hβ of Cys D). In the aliphatic region, however, only one weak NOE with a resonance at 1.11 ppm could be detected.

Signals **e** and **f** overlap at 300 K (Figure 2). However, 1D NOE difference experiments on the partially resolved peak pair at 310 K (see Figure 2, inset) unambiguously identified their individual dipolar connectivities. Resonance **e** exhibits a strong NOE to signal **j′** and a weak connectivity to a signal at 1.56 ppm. Signal **f** shows a strong NOE to signal **j″**. Both **j′** and **j″** are fast relaxing (T_1 < 10 ms) and can therefore be assigned as the geminal partners of **e** and **f**, respectively. Further NOEs of signal **f** involve resonances at 1.25 and −0.49 ppm (**z**). The latter resonance belongs to an isoleucine spin system with the δCH_3 group at −0.49 ppm (**z**). In the TOCSY and COSY spectra with slow repetition rates, **z** is correlated to Hγ protons at 1.12 and 1.40 ppm and to the Hβ at 1.35 ppm. The latter proton is connected to the γCH_3 group at 0.40 ppm (signal **y**). Dipolar connectivities in the 30 ms NOESY and in a 1D NOE difference spectrum obtained after irradiation of **z** confirm the intraresidual assignments made above. Furthermore, the methyl group **z** is in close proximity to a Hα proton at 4.38 ppm and an aromatic spin system with resonances at 7.60 and 7.35 ppm. The 2D maps suggest the assignment of the latter Hα and of the aromatic ring to the same residue with the βCH_2 protons resonating at 3.25 and 2.95 ppm, respectively. Due to the upfield shift of signal **z** it can be assumed that this methyl group is situated above or below the plane of the aromatic ring in discussion.

Signal **g** representing the seventh cluster ligand shows a broad NOE to a resonance at 9.65 ppm which is assigned to its geminal partner. Further NOE connectivities with a presumed Hα proton at 4.14 and a resonance at 1.11 ppm were detected. Signal **h** displays a similar 1D NOE difference spectrum with a connectivity to a broad resonance at 8.8 ppm (assigned to the geminal partner of **h**) and to resonances at 3.56 and 0.98 ppm. However, the latter NOE is much weaker than the strong NOE of **g** with the 1.11 ppm resonance.

Specific Assignments of the Cysteines

The structural model of PsaC derived in this work and chemical shift analogy with *C. p.* like 8Fe ferredoxins (Bertini et al., 1994) can be used to establish a sequence or position-specific assignment of all cluster ligating cysteines in PsaC. Cys C and D were already identified as the two Cys III residues of both clusters. Cys C is assigned to Cys 53 on the basis of the independent observation that resonance **c** is the first one to decrease in intensity when reduction of PsaC by dithionite is tried (Figure 3, traces a and b). Therefore, it has to belong to the more reducible cluster F_A, which was identified in previous site-directed mutagenesis studies (Zhao et al., 1992; Mehari et al., 1995) as the C-terminal cluster of PsaC. Thus, Cys D must be Cys 16 or Cys III of cluster F_B. These sequence specific assignments are also consistent with the dipolar connectivities expected for the far-shifted Hβ protons of Cys 16 and Cys 53 from the PsaC structural model. Hβ_1 Cys 16 (**d**) gives NOE to the Hα of Cys 53 and weakly to a resonance at 1.11 ppm tentatively assigned to a methyl group of Leu 25. Hβ_1 Cys 53 (**c**) is in close contact to the same methyl group of Leu 25 and to one of the methyls of Leu 62 that is therefore tentatively assigned to the resonance at 0.73 ppm experiencing 1D NOE from **c**.

After the two Cys III residues of PsaC were assigned, Cys A and B must be identified as Cys II residues due to the above mentioned characteristic chemical shift and relaxation behavior of their Hα protons. Cys A and B can be assigned as Cys 50 and Cys 13, respectively, due to their differences in chemical shift. It is a general feature of oxidized 8Fe ferredoxins that the Hβ_2 of Cys II of the C-terminal cluster

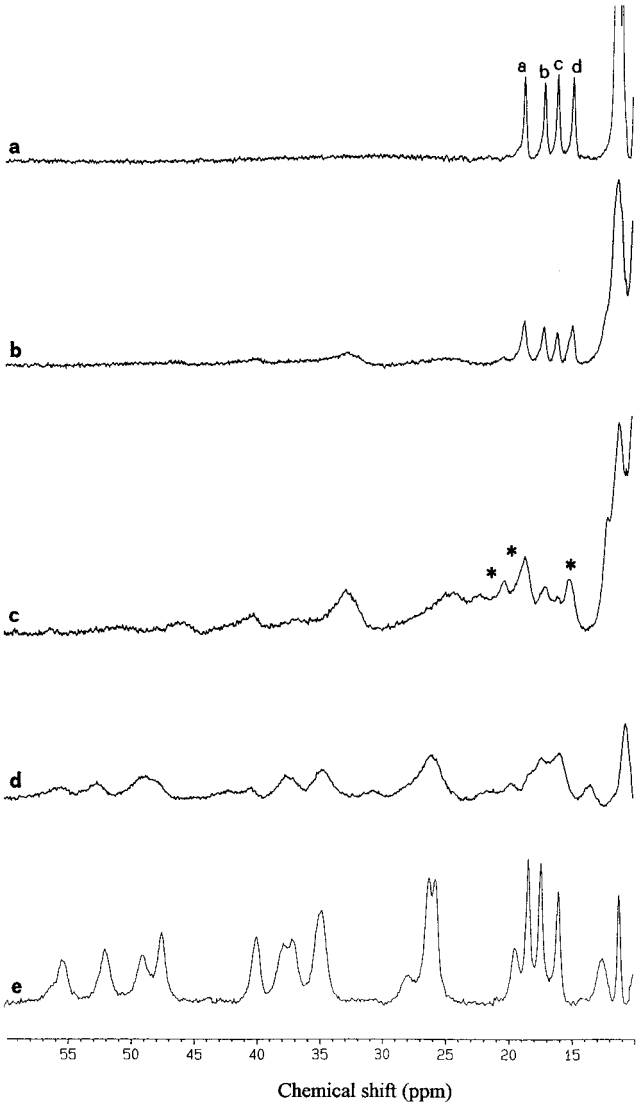

FIGURE 3: 600 MHz 1D ^{1}H NMR spectrum of oxidized (trace a), partially reduced (traces b−d), and fully reduced (trace e) PsaC from *S. elongatus*. The spectra in traces a, b, and c were recorded at 278 K, and the spectra in traces d and e were recorded at 300 K. Signals of the intermediate species that are close to the oxidized form are marked with an asterisk (*) in trace c.

is more downfield shifted than the corresponding proton of the N-terminal cluster (Bertini et al., 1994; Huber et al., 1995). The 1D NOEs of **a** and **b** with one aliphatic resonance each are then tentatively assigned to a methyl group of Val 48 (1.20 ppm) and to one of the γCH_2 protons of Ile 11 (1.23 ppm), respectively, on the basis of the PsaC structural model.

The strict conservation of a type II turn following the remote Cys IV ligand in all structurally characterized cubane ferredoxins (Bertini et al., 1995) permits the assignment of Cys G and H to the Cys IV residues of PsaC (Cys 57 and Cys 20). The turn initiates with a proline after Cys IV and is stabilized by H-bonding between the carbonyl oxygen of the latter cysteine (residue *n*) and the backbone amide proton of residue $n + 3$. Owing to this turn, the Hβ_2 of Cys IV is very close to the Hα of residue $n + 3$ so that a NOE between them is expected. As signals **g** and **h** are the only hyperfine-shifted resonances exhibiting 1D NOEs to protons in the typical Hα chemical shift range, they can be assigned to the two Cys IV residues. In the PsaC structural model, Hβ_2 Cys 57 is in the vicinity of the second methyl group of Leu 62, which could account for the strong NOE of **g** with a resonance at 1.11 ppm, whereas Hβ_2 Cys 20 has no close interresidual contacts to aliphatic protons. Therefore, we tentatively assign signal **g** to Cys 57 and signal **h** to Cys 20. Following these lines, the NOE of **g** at 4.14 ppm corresponds to Hα Asp 60 and the 3.56 ppm NOE of **h** to Hα Asp 23.

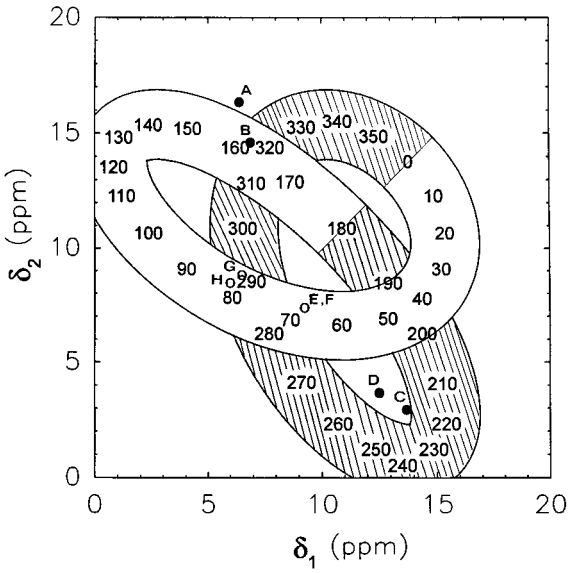

FIGURE 4: Determination of the $C_\alpha-C_\beta-S-Fe$ dihedral angles for the cysteine ligands of the two $[Fe_4S_4]^{2+}$ clusters of oxidized PsaC from *Synechococcus elongatus*. The hyperfine shifts of the βCH_2 protons, δ_1 and δ_2, were calculated from the chemical shift values in Table 1 minus 2.8 ppm (Bertini et al., 1994). Their relative relaxation rates R_1/R_2 are given by the T_1 relaxation times in Table 1 or were estimated from the linewidths in 1D and 1D NOE difference spectra. The figure depicts the relationship between δ_1 and δ_2 for various dihedral angles, as represented by numbers in the ribbon (Davy et al., 1995). The shaded part of the ribbon represents values of $R_1/R_2 < 1$, and the open ribbon values of $R_1/R_2 > 1$. Cysteines with $R_1/R_2 < 1$ (●) and cysteines with $R_1/R_2 > 1$ (○) are indicated. The indices 1 and 2 refer to the stereospecific assignments in Table 1.

At the present stage signals **e** and **f** are assigned to the Cys I ligands in PsaC by exclusion. Firm grounds for the sequence specific assignment of Cys F as Cys 10 are provided by the dipolar connectivity of **f** to the upfield-shifted methyl group **z**, which is then connected to an aromatic spin system. The latter methyl is part of an isoleucine spin system (see above). According to the PsaC model, the only pair of isoleucine−aromatic amino acid neighbors which is close enough to a Cys I ligand to account for the NOEs of **f** and **z** is Ile 6−Phe 61 in the vicinity of Cys 10. Thus, signal **e** corresponds to the remaining Cys 47 and its 1.56 ppm NOE corresponds to the side chain of Val 24. A summary of the above assignments for the cluster-coordinating cysteine residues of PsaC is given in Table 1.

In order to obtain local structural information on the geometries of the cluster ligands we have applied to PsaC a recently proposed approach to determine the $C_\alpha-C_\beta-S-Fe$ dihedral angles of cysteines coordinating $[Fe_4S_4]^{2+}$ clusters from the chemical shifts and relaxation rates of their βCH_2 protons (Bertini et al., 1994; Davy et al., 1995). The dihedral angles of most cysteine residues have values that are compatible with the previously derived relationship between the hyperfine shifts (δ_1, δ_2) of the βCH_2 protons and their relative relaxation rates R_1/R_2 (Figure 4). Minor deviations

Scheme 1

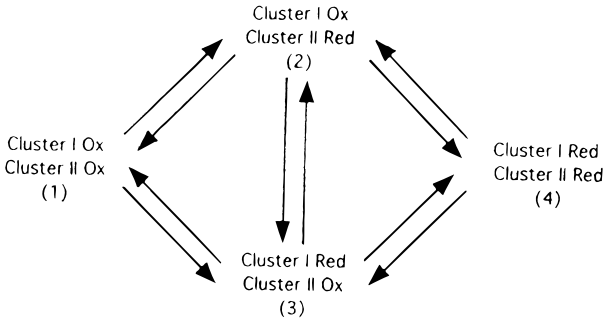

from the allowed regions of the δ_1/δ_2 plane are observed for Cys 50 (Cys A), Cys 53 (Cys C), and Cys 16 (Cys D). Nevertheless, the overall good agreement with the cysteine geometry in other $[Fe_4S_4]$ proteins confirms the structural similarity of PsaC to the smaller *C.p.* type ferredoxins serving as electron transfer proteins in solution.

Reduction of PsaC Monitored by ^{1}H NMR

The 600 MHz ^{1}H NMR spectrum of a fully reduced sample of PsaC, obtained by addition of a small amount of solid $NaBH_4$ to dithionite-reduced protein, is displayed in Figure 3e. The spectrum exhibits numerous isotropically shifted resonances in the 60−10 ppm range, typical for a reduced 4Fe or 8Fe ferredoxin. The fully reduced state of PsaC was stable for at least 4 days; after reoxidation by air the spectrum was identical to that of the oxidized species. Thus, the cycle of full (two-electron) reduction−oxidation is reversible.

Reduction of PsaC with dithionite only leads to partially reduced species in which one cluster is reduced and the other one is oxidized (cf. Scheme 1). Depending on the degree of reduction, the intermediate species exhibit resonances of oxidized PsaC, broad resonances characteristic of the intermediate reduction state, and broadened signals of the fully reduced species (Figure 3, traces b−d). By analyzing spectra b−d in more detail, it appears that the resonances of the oxidized protein in spectrum b are sizeably broader than in spectrum a and that several signals of the intermediate species appear in the same chemical shift region (peaks marked with asterisks in Figure 3c). The signals of the intermediate species are much broader than those reported for partially reduced *C.p.* and *C.au*. ferredoxin; in the latter case 2D saturation transfer experiments established a full set of correlations between the resonances of the cysteinyl cluster ligands in all three oxidation/reduction states (Bertini et al., 1992, 1994). In the present case, the strong exchange broadening of the intermediate resonances renders saturation transfer experiments not feasible and suggests strongly that the intermolecular electron transfer is in the intermediate exchange regime. From the line broadening of resonances **a**−**d** in spectra a and b (Figure 3) on the one hand and the separation in chemical shift between the intermediate and oxidized/fully reduced species on the other hand, the intermolecular electron exchange rate is estimated to be in the 10^2-10^4 s^{-1} range. Although the spectrum of the intermediate species (Figure 3c) is rather broad, it does not show evidence of two distinct one-electron reduced molecular species (i.e. one with cluster F_A reduced and F_B oxidized and vice versa; cf. Scheme 1) suggesting that the intramolecular electron exchange is faster than 10^4 s^{-1}. This would be consistent with what was observed in the case of clostridial-type ferredoxins (Bertini et al., 1992, 1994).

Attempts to slow down the intermolecular electron exchange of PsaC by lowering the temperature and raising the pH or to speed it up by addition of the mediator benzyl viologen did not appreciably improve the quality of the spectra although a narrowing of the signals was observed upon temperature decrease. Therefore, it is not possible to calculate the difference in redox potential between the two PsaC clusters from the shift ratios of the intermediate species with respect to the fully reduced and oxidized forms as done before for *C.p.* ferredoxin (Bertini et al., 1992). However, the spectra of the intermediate PsaC species display a set of signals relatively close to those of the oxidized form as well as signals relatively close to those of the fully reduced species (cf. Figure 3c and d; in Figure 3c signals close to the oxidized form are marked by an asterisk). Therefore, it is suggested that there is an appreciable difference between the microscopic reduction potentials (Bertini et al., 1990, 1994), such that the intermediate PsaC species contains a sizeably larger share of one of the two clusters (presumably F_B) in the oxidized form.

DISCUSSION

The UV/vis and EPR spectra of reconstituted PsaC characterize it as a ferredoxin with two correctly assembled $[Fe_4S_4]^{2+}$ clusters and thus confirm its identity to the native subunit of PSI. The ^{1}H NMR spectroscopic properties of unbound PsaC are in line with this result; its 1D spectrum resembles that of *C.p.* type 2$[Fe_4S_4]$ ferredoxins. The local structural information about the environment of the two clusters, obtained from 1D NOE difference experiments on the hyperfine shifted signals of PsaC, is consistent with conserved structural features of smaller 4 and 8 Fe ferredoxins and permitted a full assignment of the latter signals. Moreover, the observation of an "intercluster" NOE between signals **c** and **d** ($H\beta_1$ Cys 53 and $H\beta_1$ Cys16, respectively) clearly indicates, that the 12 Å distance between the two clusters of PsaC that was measured in the low-resolution X-ray structure of PSI (Krauss et al., 1993, 1996) is maintained in the unbound state. Thus, gross conformational differences between bound and unbound PsaC can be excluded. The $C_\alpha-C_\beta-S-Fe$ dihedral angles of the cluster ligating cysteines were determined from the chemical shifts and the relative relaxation rates of their βCH_2 protons and shown to be similar to those in $[Fe_4S_4]^{2+}$ proteins of known three-dimensional structure.

As far as the properties of reduced PsaC are concerned, there is only a qualitative similarity to *C.p.* type ferredoxins. Partial reduction of *C.p*. or *C.au*. ferredoxin gives rise to three different molecular species (Scheme 1). The two one-electron reduced species (2 and 3) are in fast exchange on the NMR time scale while the exchange rates between the fully oxidized and the two intermediate as well as between the two intermediate and the fully reduced species are slow. In the case of PsaC, the intramolecular electron exchange between species 2 and 3 seems similarly fast, as no evidence of two intermediate forms is seen in the spectra. However, the intermolecular electron exchange is close to the intermediate exchange regime (i.e. faster than in clostridial-type ferredoxins) as clearly indicated by the exchange broadening of the resonances of the intermediate species. The exchange

Table 2: Electron Exchange Rate Constants for Partially Reduced Fe−S Proteins

	PsaC	*C.p.* 8Fe ferredoxin
intramolecular	$>10^4$ s^{-1}	$>10^5$ s^{-1} [a]
intermolecular	$\approx 10^2-10^4$ s^{-1}	$>6 \times 10^2$ s^{-1} [b]

[a] Data from Bertini et al. (1992). [b] Data from Bertini et al. (1990).

rates for PsaC and *C.p.* 8Fe ferredoxin are compared in Table 2. It should be noted that *Chromatium vinosum* 8Fe ferredoxin, a 82 amino acid protein with a six amino acid insertion in the sequence of the C-terminal cluster binding motif (CxxCxxxxxxxxC as compared to CxxCxxC in PsaC and *C.p.* type ferredoxins), is so far the only 8Fe ferredoxin for which no intramolecular electron exchange at all was observed after partial reduction (Huber et al., 1995). The impeded electron transfer in this case was explained on the basis of the recent crystal structure of *C. vinosum* ferredoxin by a conformational change of the second cysteine of the C-terminal cluster and the loss of one hydrogen bond on this cluster leading to differences in the electronic structures of the clusters (Moulis et al., 1996).

Consequences for the Electron Transfer in PSI

The unbound PsaC can serve as a valid model system to predict the behavior of the photoreduced protein embedded within PSI since the redox potentials of the clusters are not significantly changed in the bound and unbound states of the protein (Yu et al., 1993). Therefore it can be anticipated that the intramolecular electron exchange between F_A and F_B will also occur in the bound state. In this context, the existence of intermolecular exchange in PsaC in solution which results in the broad, ill-defined spectra of the intermediate species is an unwanted side-effect of the model as this process will not occur in the bound state. The present NMR data is not able to yield an upper limit for the intramolecular electron exchange rate; its lower limit can be estimated to be of the order of 100 μs. It should be noted that 30 and 200 μs phases have been observed by photovoltage measurements and assigned to forward electron transfer reactions between the Fe-S clusters in PSI (Sigfriedsson et al., 1995).

The possibility of electron transfer between F_A and F_B is a necessary requirement for linear electron flow within PSI from F_X to the outermost cluster which is suggested by the relative orientation of the Fe-S clusters in the PSI X-ray structure (Krauss et al., 1993, 1996). The NMR data for unbound partially reduced PsaC suggest that this linear electron transfer scheme is indeed a possible scenario: Upon photoreduction, the electron is transferred from F_X to one of the Fe-S clusters of PsaC (most likely to the F_X-proximal cluster) and within 100 μs (or faster) both clusters F_A and F_B are partially reduced at room temperature due to fast intramolecular electron exchange. Following this step, the electron is transferred, probably via the F_X-distal cluster, to the acceptor proteins ferredoxin or flavodoxin. The immediate donor to the acceptor protein may be both F_A or the less reducible cluster F_B since the electron is exchanged fast between F_A and F_B. Thus, electron transfer to the acceptor proteins is possible via both clusters as long as the overall thermodynamics of the process is favorable. The argument against an assignment of F_B as the outermost PSI cluster based on thermodynamic grounds may thus not be valid anymore. The reduction behavior of the unbound PsaC in solution, of course, only suggests that such a linear pathway is, in principle, possible. The true electron transfer pathway through the terminal Fe-S clusters in PSI remains to be determined by different techniques.

ACKNOWLEDGMENT

We thank Prof. Stefano Mangani (University of Siena) for help with the construction of the structural model and with the SYBYL program.

SUPPORTING INFORMATION AVAILABLE

1D NOE difference spectra obtained by selective irradiation of the hyperfine shifted resonances of oxidized PsaC in D_2O solution (Figures S1 and S2); temperature dependence of the hyperfine shifted resonances of oxidized PsaC in a chemical shift *vs* $1/T$ plot (Figure S3) (5 pages). Ordering information is given on any current masthead page.

REFERENCES

Adman, E. T., Sieker, L. C., & Jensen, L. H. (1973) *J. Biol. Chem. 248*, 3987.

Adman, E. T., Sieker, L. C., & Jensen, L. H. (1976) *J. Biol. Chem. 251*, 3801.

Armengaud, J., Gaillard, J., Forest, E., & Jouanneau, Y. (1995) *Eur. J. Biochem. 231*, 396.

Babini, E., Bertini, I., Borsari, M., Capozzi, F., Dikiy, A., Eltis, L. D., & Luchinat, C. (1996) *J. Am. Chem. Soc. 118*, 75.

Banci, L., Bertini, I., Luchinat, C., Piccioli, M., Scozzafava, A., & Turano, P. (1989) *Inorg. Chem. 28*, 4650.

Banci, L., Bertini, I., Ciurli, S., Ferretti, S., Luchinat, C., & Piccioli, M. (1993) *Biochemistry 32*, 9387.

Bertini, I., & Luchinat, C. (1996a) in *Transition metal sulfur chemistry: biological and industrial significance* (Stiefel, E. I., & Matsumoto, K. Eds.) pp 57−73, ACS Symposium Series 653, American Chemical Society, Washington, DC.

Bertini, I., & Luchinat, C. (1996b) in *NMR of paramagnetic substances*, Coordination Chemistry Reviews 150, Elsevier, Amsterdam.

Bertini, I., Briganti, F., Luchinat, C., & Scozzafava, A. (1990) *Inorg. Chem. 29*, 1874.

Bertini, I., Briganti, F., Luchinat, C., Messori, L., Monnanni, R., Scozzafava, A., & Vallini, G. (1992) *Eur. J. Biochem. 204*, 831.

Bertini, I., Capozzi, F., Luchinat, C., Piccioli, M., & Vila, A. J. (1994) *J. Am. Chem. Soc. 116*, 651.

Bertini, I., Donaire, A., Feinberg, B. A., Luchinat, C., Piccioli, M., & Yuan, H. (1995) *Eur. J. Biochem. 232*, 192.

Bertini, I., Luchinat, C., & Rosato, A. (1996) *Prog. Biophys. Mol. Biol. 66*, 43.

Brettel, K. (1997) *Biochim. Biophys. Acta 1318*, 322.

Chen, Z. G., de Ropp, J. S., Hernandez, G., & La Mar, G. N. (1994) *J. Am. Chem. Soc. 116*, 8772.

Davy, S. L., Osborne, J. M., Breton, J., Moore, G. R., Thomson, A. J., Bertini, I., & Luchinat, C. (1995) *FEBS Lett. 363*, 199.

Donaire, A., Gorst, C. M., Zhou, Z. H., Adams, M. W. W., & La Mar, G. N. (1994) *J. Am. Chem. Soc. 116*, 6841.

Duée, E. D., Fanchon, E., Vicat, J., Sieker, L. C., Meyer, J., & Moulis, J.-M. (1994) *J. Mol. Biol. 243*, 683.

Dunn, P. P. J., & Gray, J. C. (1988) *Plant Mol. Biol. 11*, 311.

Fukuyama, K., Nagahara, Y., Tsukihara, T., & Katsube, Y. (1988) *J. Mol. Biol. 199*, 183.

Golbeck, J. H. (1994) in *Advances in photosynthesis: The molecular biology of cyanobacteria* (Bryant, D. A., Ed.) pp 319−360, Kluwer Academic Publishers, Dordrecht, The Netherlands.

Griesinger, C., Otting, G., Wüthrich, K., & Ernst, R. R. (1988) *J. Am. Chem. Soc. 110*, 7870.

He, W. Z., & Malkin, R. (1994) *Photosyn. Res. 41*, 381.

Heathcote, P., William-Smith, D. L., Sihra, C. K., & Evans, M. (1978) *Biochim. Biophys. Acta 503*, 333.

Huber, J. G., Gaillard, J., & Moulis, J.-M. (1995) *Biochemistry 34*, 194.
Inubushi, T., & Becker, E. D. (1983) *J. Magn. Reson. 51*, 128.
Johnson, R. D., Ramaprasad, S., & La Mar, G. N. (1983) *J. Am. Chem. Soc. 105*, 7205.
Jung, Y. S., Yu, L., & Golbeck, J. H. (1995) *Photosyn. Res. 46*, 249.
Kissinger, C. R., Sieker, L. C., Adman, E. T., & Jensen, L. H. (1991) *J. Mol. Biol. 219*, 693.
Krauss, N., Hinrichs, W., Witt, I., Fromme, P., Pritzkow, W., Dauter, Z., Betzel, C., Wilson, K. S., Witt, H. T., & Sänger, W. (1993) *Nature 361*, 326.
Krauss, N., Schubert, W. D., Klukas, O., Fromme, P., Witt, H. T., & Sänger, W. (1996) *Nat. Struct. Biol. 3*, 965.
Laskowski, R. A., MacArthur, M. W., Moss, D. S., & Thornton, J. M. (1993) *J. Appl. Crystallogr. 26*, 283.
Leibl, W., Toupance, B., & Breton, J. (1995) *Biochemistry 34*, 10237.
Li, N., Zhao, J., Warren, P. V., Warden, J. T., Bryant, D. A., & Golbeck, J. H. (1991) *Biochemistry 30*, 7863.
Macedo-Ribeiro, S., Darimont, B., Sterner, R., & Huber, R. (1996) *Structure 4*, 1291.
Marion, D., & Wüthrich, K. (1983) *Biochem. Biophys. Res. Commun. 113*, 967.
Mehari, T., Parrett, K. G., Warren, P. V., & Golbeck, J. H. (1991) *Biochim. Biophys. Acta 1056*, 139.
Mehari, T., Qiao, F., Scott, M. P., Nellis, D. F., Zhao, J., Bryant, D. A., & Golbeck, J. H. (1995) *J. Biol. Chem. 270*, 28108.
Moulis, J.-M., Sieker, L. C., Wilson, K. S., & Dauter, Z. (1996) *Protein Sci. 5*, 1765.
Mühlenhoff, U., Haehnel, W., Witt, H., & Herrmann, R. G. (1993) *Gene 127*, 71.
Oh-oka, H., Takahashi, Y., Kuriyama, K., Saeki, M., & Matsubara, H. (1988a) *J. Biochem. 103*, 962.
Oh-oka, H., Takahashi, Y., Matsubara, H., & Ito, S. (1988b) *FEBS Lett. 234*, 291.
Packer, E. L., Sternlicht, H., Lode, E. T., & Rabinowitz, J. C. (1975) *J. Biol. Chem. 250*, 2062.
Pearlman, D. A., Case, D. A., Caldwell, G. C., Siebel, G. L., Singh, U. C., Weiner, P., & Kollman, P. A. (1991) *AMBER4.0*, University of California, S. Francisco, CA.
Rance, M., Sørensen, O. W., Bodenhausen, G., Wagner, G., Ernst, R. R., & Wüthrich, K. (1983) *Biochem. Biophys. Res. Commun. 117*, 479.
Sery, A., Housset, D., Serre, L., Bonicel, J., Hatchikian, C., Frey, M., & Roth, M. (1994) *Biochemistry 33*, 15408.
Sigfriedsson, K., Hansson, T. M., & Brzezinski, P. (1995) *Proc. Natl. Acad. Sci. U.S.A. 92*, 3458.
Stout, C. D. (1989) *J. Mol. Biol. 205*, 545.
Stout, C. D. (1993) *J. Biol. Chem. 268*, 25920.
Studier, F. W., Rosenberg, A. H., Dunn, J. J., & Dubendorff, J. W. (1990) *Methods Enzymol. 185*, 60.
Vold, R. L., Waugh, J. S., Klein, M. P., & Phelps, D. E. (1968) *J. Chem. Phys. 48*, 3831.
Wider, G., Macura, S., Kumar, A., Ernst, R. R., & Wüthrich, K. (1984) *J. Magn. Reson. 56*, 207.
Yu, L., Zhao, J., Lu, W., Bryant, D. A., & Golbeck, J. H. (1993) *Biochemistry 32*, 8251.
Zhao, J., Li, N., Warren, P. V., Golbeck, J. H., & Bryant, D. A. (1992) *Biochemistry 31*, 5093.

BI9714058